J. Fluid Mech. (2006), *vol.* 561, *pp.* 417–437.
doi:10.1017/S0022112006000942 Printed in the United Kingdom

Three-dimensional instabilities of periodic gravity waves in shallow water

By MARC FRANCIUS AND CHRISTIAN KHARIF

Institut de Recherche sur les Phénomènes Hors-Equilibre, Technopôle de Château-Gombert, 49 Rue Frédéric Joliot-Curie, B P 146, 13384 Marseille Cedex 13, France

(Received 22 March 2005 and in revised form 25 January 2006)

A linear stability analysis of finite-amplitude periodic progressive gravity waves on water of finite depth has extended existing results to steeper waves and shallower water. Some new types of instability are found for shallow water. When the water depth decreases, higher-order resonances lead to the dominant instabilities. In contrast with the deep water case, we have found that in shallow water the dominant instabilities are usually associated with resonant interactions between five, six, seven and eight waves. For small steepness, dominant instabilities are quasi two-dimensional. For moderate and large steepness, the dominant instabilities are three-dimensional and phased-locked with the unperturbed nonlinear wave. At the margin of instability diagrams, these results suggest the existence of new bifurcated three-dimensional steady waves.

1. Introduction

This paper deals with the study of the stability of finite-amplitude two-dimensional periodic gravity waves of permanent form in water of uniform depth with respect to two- and three-dimensional infinitesimal disturbances. There have been extensive studies on the stability of periodic waves in shallow water. Yet, for most of these studies whether analytic or semi-numerical, the validity of their analysis is limited by the assumption of weak nonlinearity of the travelling periodic waves.

Whitham (1965) applied the averaged variational approach to the Korteweg–de Vries (KdV) equation and the Boussinesq equation, and found that periodic cnoidal waves are stable to two-dimensional modulational disturbances. A stability analysis for the Stokes wave was done by Infeld & Rowlands (1979) and Infeld (1980), by using the Kamdomtsev–Pietvaschvili (KP) equation, a generalization of the KdV equation, and different forms of the Boussinesq equation to account for weak three-dimensional effects. Except for the KP equation for which periodic wave are stable, these models yield dominant instabilities that are three-dimensional. The obliqueness and the growth rate of these instabilities decrease with decreasing depth. All these works consider periodic disturbances of wavelength much greater than the fundamental wavelength of the Stokes wave, hence they include only modulational perturbations. Besides, these results should be considered with care, because the validity of the Stokes' representation for shallow water is questionable. Nevertheless, using Whitham's theory, Infeld & Rowlands (1990) found that the cnoidal wave solutions of the KP equation are stable to periodic three-dimensional long or modulational perturbations.

A unified approach was developed by Bryant (1974, 1978), who used truncated Euler equations to compute weakly nonlinear periodic progressive waves without

restriction on kh, and also to study their stability to periodic two- and three-dimensional disturbances of greater or equal wavelength. Bryant (1978) reported three-dimensional instabilities associated with the lowest-order possible resonance for gravity waves, namely the second-order quartet wave resonance between the basic wave and the disturbances. No evidence was found for linear instability of disturbances with wavelength equal to the fundamental wavelength, either in the case of two-dimensional disturbances or in the three-dimensional case. However, in the two-dimensional case, Bryant (1974) found that when the unperturbed waves are more strongly nonlinear or when the disturbances have wavelength large compared with the fundamental wavelength, the margin of stability of the disturbances decreases so that the unperturbed waves were in practice only marginally stable.

Using the full exact equations, McLean (1982*b*) investigated the next-order resonance, and introduced a classification of the corresponding instabilities according to the number of waves associated with the corresponding resonant condition. The class I and class II instabilities correspond, respectively, to an even and an odd number of resonant waves. The second-order resonance corresponds to quartet-wave interactions and belongs to class I. The third-order resonance corresponds to quintet-wave interactions and belongs to class II. The third-order resonance was also analysed by Stiassnie & Shemer (1984) who used the Zakharov integral equation up to fourth order in the wave steepness. For non-dimensional depth $kh \geqslant 0.365$, their stability results were in agreement with McLean's results, although the instability region of class I was found to consist of two disconnected domains. The authors suggested that these differences might be a result of the perturbation expansions used in their analytical studies. McLean (1982*b*) considered three depths, one greater and two smaller than the bifurcation value $kh = 1.363$. For small amplitudes and all depths, he found that the second-order resonance dominates. In the shallowest case, $kh \approx 0.5$, he investigated, the corresponding dominant instability is two-dimensional with a wavelength comparable to the fundamental wavelength. For moderate steepness, the dominant instability shifts to three-dimensional and is still associated with the second-order resonance. For sufficiently steep waves, the third-order resonance dominates and the most unstable disturbance is three-dimensional.

The major motivation of the present work is to extend the results of Bryant (1978), McLean (1982*b*) and Stiassnie & Shemer (1984) to greater steepness and to shallower water. The rest of the paper is organized as follows. In § 2, the governing equations are presented for the description of the nonlinear wave and for the linear instability analysis. The analysis proceeds along the lines of the finite-depth case treated by McLean (1982*b*). The nonlinear wave is computed with the iterative method of Longuet-Higgins (1988) and the eigenvalue system is generated using a Galerkin method proposed by Zhang & Melville (1987) to study the stability of gravity–capillary waves on deep water. In § 3, numerical results are presented for small and large to moderate steepness. The discovered phased-locked stationary disturbances associated with higher-order resonances suggest the existence of new steady three-dimensional waves, which might bifurcate from the two-dimensional unperturbed wave. The symmetry properties of the bifurcated surface patterns are examined. In § 4, conclusions are drawn.

2. Governing equations

The fluid is assumed to be inviscid and the motion irrotational, so the velocity $\boldsymbol{u}$ may be expressed as the gradient of a potential ϕ: $\boldsymbol{u} = \nabla\phi$. If the fluid is assumed to

be incompressible, such that $\nabla \cdot \boldsymbol{u} = 0$, the equation that holds throughout the fluid is Laplace's equation

$$\nabla^2 \phi = 0 \quad \text{for} \quad -h < z < \eta(x, y, t), \tag{2.1}$$

where x and y are coordinates in the horizontal plane, and the z-axis is positive upwards. The surface elevation is given by $z = \eta(x, y, t)$ and the horizontal bottom is located at $z = -h$. The bottom condition is

$$\frac{\partial \phi}{\partial z} = 0 \quad \text{on} \quad z = -h. \tag{2.2}$$

The kinematic requirement that a particle on the free surface remains on it is expressed by

$$\frac{\partial \eta}{\partial t} + \frac{\partial \phi}{\partial x}\frac{\partial \eta}{\partial x} + \frac{\partial \phi}{\partial y}\frac{\partial \eta}{\partial y} - \frac{\partial \phi}{\partial z} = 0 \quad \text{on} \quad z = \eta(x, y, t). \tag{2.3}$$

The dynamic boundary condition can be written

$$\frac{\partial \phi}{\partial t} + \tfrac{1}{2}(\nabla \phi)^2 + g\eta + \frac{p_a}{\rho} = B(t) \quad \text{on} \quad z = \eta(x, y, t), \tag{2.4}$$

where g is the acceleration due to gravity, p_a the pressure at the free surface, ρ the density of the fluid and $B(t)$ is a function independent of spatial coordinates due to the integration. This function constant can always be eliminated by redefining the velocity potential by $\partial \Phi / \partial t = \partial \phi / \partial t - B(t)$. Air motion is not taken into account and the pressure at the free surface p_a may be taken as equal to zero without loss of generality. Surface tension effects are ignored.

The computations consist of two parts, calculation of the unperturbed wave followed by a normal mode analysis of unsteady linear equations for the perturbations. We normalize the equations by choosing $k = 1$, $g = 1$ and work with non-dimensional variables. The normalized wavelength is $\lambda = 2\pi$.

2.1. *Steady solutions*

We consider two-dimensional gravity waves propagating steadily at the free surface. In the frame of reference moving with the wave, the governing equations become

$$\nabla^2 \overline{\phi} = 0 \quad \text{for} \quad -h < z < \overline{\eta}, \tag{2.5}$$

$$\frac{\partial \overline{\phi}}{\partial z} = 0 \quad \text{on} \quad z = -h, \tag{2.6}$$

$$\frac{\partial \overline{\phi}}{\partial x}\frac{\partial \overline{\eta}}{\partial x} - \frac{\partial \overline{\phi}}{\partial z} = 0 \quad \text{on} \quad z = \overline{\eta}, \tag{2.7}$$

$$\tfrac{1}{2}(\nabla \overline{\phi})^2 + \overline{\eta} = C \quad \text{on} \quad z = \overline{\eta}, \tag{2.8}$$

where C is a constant of the wave motion. Following Longuet-Higgins (1988), we chose for computational convenience the origin of z at a level such that the right-hand side of equation (2.8) is zero. This implies that the zero level is somewhat above the wave crest.

Since the stability analysis requires highly accurate computation of the nonlinear periodic waves $(\overline{\eta}, \overline{\phi})$, we used the method developed by Longuet-Higgins (1988). At the surface the streamfunction $\overline{\psi} = 0$, and at the bottom $\overline{\psi} = \Psi_b$. The free surface

can be expressed in the form

$$\overline{\eta} = \tfrac{1}{2}a_o + \sum_{n=1}^{\infty} a_n \cos\left(\frac{n\overline{\phi}}{c}\right), \tag{2.9}$$

where c is the wave speed. Once the steepness and the undisturbed depth $h = \Psi_b/c$ are fixed, the unknown coefficients a_n are computed by the method of Longuet-Higgins (1988). In the chosen reference frame, the undisturbed water depth h corresponds to the depth of an uniform flow with the same momentum as the nonlinear wave. Then the mean depth is given by

$$\overline{h} = h + K, \tag{2.10}$$

where the quantity K is given by

$$K = \tfrac{1}{2}\sum_{n=1}^{\infty} n\gamma_n a_n^2, \tag{2.11}$$

with

$$\gamma_o = 1, \qquad \gamma_n = \operatorname{cotanh}\frac{n\Psi_b}{c}, \qquad n = 1, 2, \ldots.$$

In order to compute the coefficients a_n, one should truncate the Fourier series (2.9) at a given order N, and fix a value for the undisturbed depth h and the wave steepness

$$ak = a_1 + a_3 + a_5 + \cdots + a_N. \tag{2.12}$$

By using the free-surface conditions as formulated by Longuet-Higgins (1988), we obtain a system of N nonlinear algebraic equations which can easily be solved iteratively by Newton's method. The determination of the potential and its derivatives is a separate problem. The potential at the free surface is computed by solving iteratively the following equation

$$x = -\frac{\overline{\phi}}{c} - \sum_{n=1}^{N} a_n\gamma_n \sin\left(\frac{n\overline{\phi}}{c}\right), \tag{2.13}$$

and its derivatives are computed with the Cauchy–Riemman relations.

2.2. *Stability of the steady solutions*

We consider basic steady solutions with wavenumber $k = 1$. For the linear stability analysis, the reference frame is again one moving at the speed of the wave, but one in which the mean level of the nonlinear wave is zero and the bottom is located at $z = -\overline{h}$. In this reference frame, we study the stability of finite-amplitude waves subject to infinitesimal three-dimensional disturbances and let

$$\eta(x, y, t) = \overline{\eta}(x) + \eta'(x, y, t), \tag{2.14}$$

$$\phi(x, y, z, t) = \overline{\phi}(x, z) + \phi'(x, y, z, t), \tag{2.15}$$

where $(\overline{\eta}, \overline{\phi})$ and (η', ϕ') correspond, respectively, to the unperturbed wave and the infinitesimal disturbances ($|\eta'| \ll |\overline{\eta}|$, $|\phi'| \ll |\overline{\phi}|$). We substitute (2.14) and (2.15) into (2.7) and (2.8). Linearization of the equations about $z = \overline{\eta}$ yields linear evolution equations for the disturbances

$$\frac{\partial\eta'}{\partial t} + \frac{\partial\overline{\phi}}{\partial x}\frac{\partial\eta'}{\partial x} + \frac{\partial\overline{\eta}}{\partial x}\frac{\partial\phi'}{\partial x} + \left(\frac{\partial^2\overline{\phi}}{\partial x\partial z}\frac{\partial\overline{\eta}}{\partial x} - \frac{\partial^2\overline{\phi}}{\partial z^2}\right)\eta' - \frac{\partial\phi'}{\partial z} = 0, \tag{2.16}$$

$$\frac{\partial \phi'}{\partial t} + \eta' + \frac{\partial \overline{\phi}}{\partial x}\frac{\partial \phi'}{\partial x} + \frac{\partial \overline{\phi}}{\partial z}\frac{\partial \phi'}{\partial z} + \left(\frac{\partial^2 \overline{\phi}}{\partial x \partial z}\frac{\partial \overline{\phi}}{\partial x} + \frac{\partial^2 \overline{\phi}}{\partial z^2}\frac{\partial \overline{\phi}}{\partial z}\right)\eta' = 0, \tag{2.17}$$

which are to be satisfied on the unperturbed free surface $z = \overline{\eta}$. Furthermore the potential ϕ' satisfies the Laplace equation on the domain defined by $-\overline{h} < z < \overline{\eta}$ and the bottom condition $\partial\phi'/\partial z = 0$ at $z = -\overline{h}$.

Non-trivial solutions of the linearized problem corresponding to equations (2.16) and (2.17) are sought in the form

$$\eta' = \mathrm{e}^{-\mathrm{i}\sigma t}\mathrm{e}^{\mathrm{i}(px+qy)}\sum_{-\infty}^{\infty} a_j \mathrm{e}^{\mathrm{i}jx}, \tag{2.18}$$

$$\phi' = \mathrm{e}^{-\mathrm{i}\sigma t}\mathrm{e}^{\mathrm{i}(px+qy)}\sum_{-\infty}^{\infty} b_j \frac{\mathrm{ch}(k_j(z+\overline{h}))}{\mathrm{ch}(k_j\overline{h})}\mathrm{e}^{\mathrm{i}jx}, \tag{2.19}$$

where $k_j = \sqrt{(p+j)^2+q^2}$ corresponds to the modulus of the wave vector $\boldsymbol{k}_j = (p+j, q)^t$. Expressions (2.18) and (2.19) have the form of a periodic function of x, with the same wavelength as the undisturbed wave, multiplied by a periodic function of x with wavelength $2\pi/p$, a periodic function of the transverse coordinate y with transverse wavelength $2\pi/q$, and an exponential function of time. The numbers p and q are arbitrary real numbers.

Substitution of (2.18) and (2.19) into the linearized equations (2.16) and (2.17) yields a generalized eigenvalue problem for σ which, after truncation at M Fourier modes, can be written in the general form

$$\boldsymbol{A}u = \sigma \boldsymbol{B}\boldsymbol{u}, \tag{2.20}$$

where $\boldsymbol{u} = (a_{-M} \ldots a_M, b_{-M} \ldots b_M)^t$ represents the corresponding eigenvector. The matrices $\boldsymbol{A}$ and $\boldsymbol{B}$ are complex functions of p, q, as well as mean depth $\overline{h}$ and wave steepness ak of the unperturbed wave. Thus σ_n are the unknown discrete eigenvalues to be determined, and $(a_{nj}, b_{nj})^t$ their associated eigenvector, for n in $(-M, M)$ and j in $(-M, M)$. Because the water-wave system has an underlying Hamiltonian structure, eigenvalues must appear as either pure real or complex-conjugate pairs. Instability corresponds to $\mathrm{Im}(\sigma_n) > 0$ for at least one mode n, given the values of p and q.

The spectrum is easy to compute when $ak = 0$ (flat surface). Then the mean depth $\overline{h}$ is equal to the undisturbed depth h since $K = 0$, and all the eigenvalues are real

$$\sigma_n^{\pm} = -c_0(p+n) \pm [k_n \tanh(k_n h)]^{1/2}, \tag{2.21}$$

where $c_0 = \sqrt{\tanh(h)}$ and $k_n = \sqrt{(p+n)^2+q^2}$. They represent progressive waves (marginally stable disturbances) propagating on a uniform flow with potential $\overline{\phi} = -c_0 x$. The sign $\pm$ gives the direction of propagation of the perturbation relative to the unperturbed wave. To investigate the effect of finite-amplitude on this set of eigenvalues, MacKay & Saffman (1986) used a powerful theorem on the stability of equilibria of Hamiltonian systems. This theorem states that the unperturbed wave can lose spectral stability with finite-amplitude effects, if two simple eigenvalues coalesce with opposite signature or at zero frequency. The signature is defined as sign $[\pm\mathrm{Im}(-\mathrm{i}\sigma^{\pm})]$. In fact for pure gravity waves, degenerate eigenvalues with opposite signatures exist for $ak = 0$. Thus small nonlinear effects are expected to produce bands of instability in the neighbourhood of the loci of collisions of the eigenvalues. The loci of collisions define two families of curves in the (p, q)-plane: class I when the collisions occur between modes with $\sigma_m^+ = \sigma_{-m}^-$, and class II when the collisions occur

between modes with $\sigma_m^+ = \sigma_{-m-1}^-$. The corresponding instabilities are called class I and class II instabilities with the integer $m \geqslant 1$. The linear resonance conditions, namely when $ak = 0$, are for class I,

$$\sqrt{k_m \tanh(k_m h)} + \sqrt{k_{-m} \tanh(k_{-m} h)} = 2mc_0, \tag{2.22}$$

and for class II,

$$\sqrt{k_m \tanh(k_m h)} + \sqrt{k_{-m-1} \tanh(k_{-m-1} h)} = (2m+1)c_0. \tag{2.23}$$

These relations can also be written in the fixed frame of reference,

$$n\boldsymbol{k}_0 = \boldsymbol{k}_1 + \boldsymbol{k}_2, \tag{2.24}$$

$$n\omega_0 = \omega_1 + \omega_2, \tag{2.25}$$

where $n = 2, 3, \ldots$ represents the order of resonance and also the number of harmonics of the unperturbed wave with fundamental wavenumber $\boldsymbol{k}_0 = (1, 0)$ that is in resonance with the two perturbations having wavenumbers $\boldsymbol{k}_1$ and $\boldsymbol{k}_2$. Here $\omega_i = \sqrt{|\boldsymbol{k}_i| \tanh(|\boldsymbol{k}_i| h)}$ is the linear dispersion relation for gravity waves. Thus $n = 2$ corresponds to quartet resonant interactions, with $\boldsymbol{k}_1 = (1+p, q)^t$ and $\boldsymbol{k}_2 = (1-p, -q)^t$. Next, $n = 3$ corresponds to quintet resonant interactions, with $\boldsymbol{k}_1 = (1+p, q)^t$ and $\boldsymbol{k}_2 = (2-p, -q)^t$. The eigenvalues σ are computed by using an eigenvalue solver based on a 'QZ' algorithm. For details of the numerical aspects of the method, see McLean (1982*b*) and Zhang & Melville (1987).

3. Numerical results

The stability of finite-amplitude periodic gravity waves was studied for various values of steepness and depth $h < \pi/4$. Following the work of Fenton (1979), we choose to refer to shallow water waves when $kh < \pi/4$. Fenton (1979) obtained fifth-order and ninth-order cnoidal wave solutions, and compared these high-order cnoidal wave solutions with the fifth-order Stokes wave solutions and the exact numerical results of Cokelet (1977). From this analysis, he found that a boundary of applicability between deep- and shallow-water theories could be drawn near $\lambda/h \approx 8$ or $kh \approx \pi/4$.

First, we consider the stability of small-amplitude waves in shallow-water, and adopt the approach of Bryant (1978) by considering the effects of decreasing depth for a fixed value of the shallow water parameter a/h. Then, in § 3.2, we analyse in detail the stability of strongly nonlinear waves for the two cases $h = 0.5$ and $h = 0.3$. We have re-examined the case $h = 0.5$, since we have found the results of McLean (1982*b*) incomplete for moderate to large steepness. The maximum growth rates of the instabilities associated with the resonances $n = 2, 3, 4, 5, 6$ and 7 are analysed for a large range of values of the steepness ak. Finally, in § 3.3, we discuss the implications of the discovered disturbances that are stationary relative to the unperturbed wave and are associated with the $n = 4, 5, 6, 7$ resonances. Indeed, this suggests the occurrence of bifurcations from the two-dimensional unperturbed wave into steady three-dimensional waves. The symmetry properties of these probable bifurcated waves are briefly discussed.

A discussion on the accuracy of the numerical results and efficiency of the method is presented in the Appendix.†

† This appendix is available as a supplement to the online version of the paper, or from the Journal of Fluid Mechanics Editorial Office.

kh	ak	c^2	$\overline{h}$	$(a/h)/(kh)^2$
0.50	0.0250	0.46814690	0.50065899	0.20
0.30	0.0150	0.29930575	0.30035132	0.55
0.25	0.0125	0.25336472	0.25027500	0.80
0.10	0.0050	0.10639908	0.10006225	5.00

TABLE 1. Characteristics of the unperturbed waves with $a/h = 0.05$.

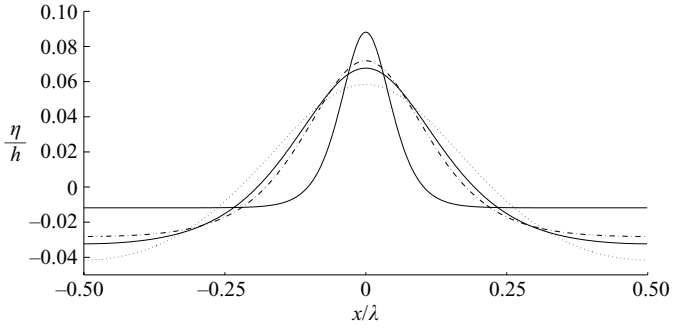

FIGURE 1. One wavelength profile for four values of $h(\epsilon_s = 0.05)$. $h = 0.5$ $(\cdots)$; $h = 0.3$ (—); $h = 0.25$ (—·—); $h = 0.1$ (—).

3.1. *Finite-depth effects for small nonlinearity*

To our knowledge, there exist few results on the stability of cnoidal-like waves. Here, cnoidal-like waves refer to fairly long periodic surface waves on water of uniform depth, such as the cnoidal solution of the KdV equation or the Boussinesq equation that are examples of first-order approximations to periodic travelling waves in shallow water. Using Whitham's theory, Infeld & Rowlands (1990) found that the cnoidal wave solutions of the KP equation are stable to periodic three-dimensional long or modulational perturbations. Using a truncated form of the Euler equations, Bryant (1974, 1978) studied the stability of nonlinear periodic waves, subject to periodic two- and three-dimensional disturbances of greater or equal wavelength. He found stability for two-dimensional disturbances and instability for certain three-dimensional disturbances. No evidence was found for linear instability of disturbances with wavelength equal to the fundamental wavelength.

Following the idea of Bryant (1978), we analysed the stability of waves with a fixed shallow-water amplitude $a/h = 0.05$ and decreasing value of the undisturbed depth h. Equivalently, decreasing value of h may be interpreted as an increase in wavelength of the unperturbed wave. In Bryant's analysis, shallow-water scalings are used and the two parameters describing the nonlinear wave are the nonlinear shallow-water parameter a/h and the non-dimensional depth $\mu = kh$ with $k = 1$. In our numerical study, we chose to use the same scaling as McLean (1982*b*) and consider the steepness $ak = \mu\, a/h$ as the varying nonlinear parameter, the non-imensional undisturbed depth being $\mu = kh$. Thus, our results scale as $\mathrm{Im}(\sigma) = ak\sqrt{kh}\,\mathrm{Im}(\sigma_B)$, where the index B refers to Bryant's scalings. We have studied four waves whose properties are given in table 1. It is well known that weakly nonlinear permanent shallow-water waves are possible if $a/h \sim (kh)^2$, when amplitude and frequency dispersion effects are in balance. Figure 1 shows the corresponding wave profiles. Bryant's results concern mainly the cases $h = 0.5$ and $h = 0.25$.

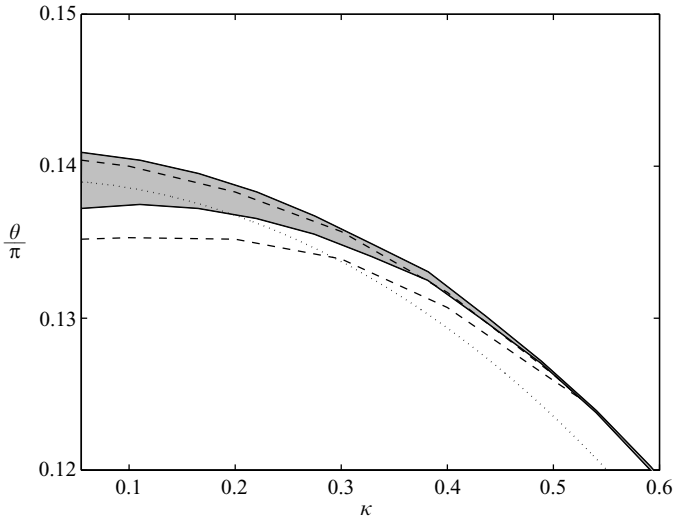

FIGURE 2. Primary region of class I ($n=2$) instability for $a/h=0.05$ and $h=0.5$. The boundaries are given by the solid lines and the dotted line is the curve of linear resonance. Bryant's results are shown by dashed lines.

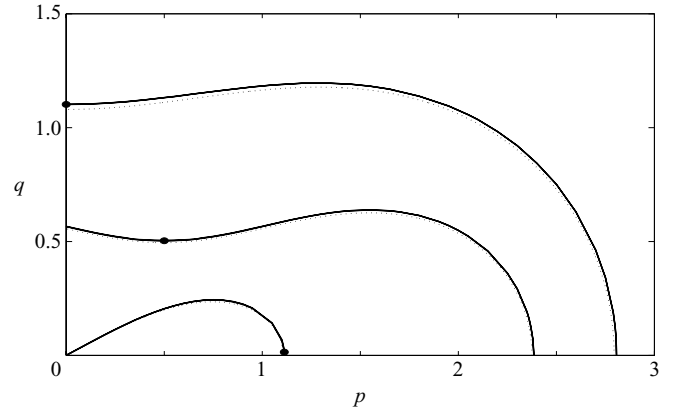

FIGURE 3. Diagram of instability for $a/h=0.05$ and $h=0.5$. Unstable regions for the resonances $n=2, 3, 4$. The dots label the most unstable modes of each region of instabilities. The dotted lines represent the resonance curves.

For $h=0.5$, figure 2 shows the class I ($n=2$) instability region (shaded zone) in the (κ-θ)-plane with $\kappa=\sqrt{p^2+q^2}$ and $\theta=a\tan(q/p)$. The present results are shown by solid lines while Bryant's results are dashed lines. The region of instability is thinner than predicted by Bryant, the upper boundary being in closer agreement with the present numerical results than the lower boundary. Besides, the region of instability computed by Bryant does not extend beyond a certain wavenumber with modulus $\kappa\approx0.523$, which corresponds to an oblique disturbance with $\theta\approx0.125\pi$. Our numerical results show that class I ($n=2$) instabilities exist for greater values of κ, but for less oblique disturbances. In particular, in the (p,q)-plane, two-dimensional instabilities exist for a very thin region $1.1119<p<1.1133$ ($q=0$). The most unstable two-dimensional disturbance has a growth rate comparable with that of the most unstable three-dimensional disturbance, which is located near $(p,q)=(1.112, 0.015)$ (see figure 3). In fact, the class I ($n=2$) instability region presents two local maxima

		Class I ($n=2$)				Class II ($n=3$)			
h	ak	p	q	Re σ	Im σ	p	q	Re σ	Im σ
0.50	0.0250	1.1126	0	−0.157	3.57×10^{-4}	0.5	0.504	0	1.62×10^{-4}
0.30	0.0150	1.0558	0	−0.061	1.95×10^{-4}	2.1859	0.0182	−0.203	1.75×10^{-4}
0.25	0.0125	1.0457	0.0079	−0.046	1.49×10^{-4}	2.144	0.0151	−0.145	1.74×10^{-4}
0.10	0.0050	1.029	0	−0.018	0.33×10^{-4}	2.0176	0.016	−0.042	0.63×10^{-4}

TABLE 2. Maximum growth rate for resonances $n=2, 3$. The unperturbed waves have the same value $a/h=0.05$ for various depths.

		Class I ($n=4$)				Class II ($n=5$)			
h	ak	p	q	Re σ	Im σ	p	q	Re σ	Im σ
0.50	0.0250	0	1.102	0	0.54×10^{-4}	—	—	—	—
0.30	0.0150	0	0.677	0	0.83×10^{-4}	—	—	—	—
0.25	0.0125	2.3203	0.0195	−0.321	1.18×10^{-4}	—	—	—	—
0.10	0.0050	2.113	0.0258	−0.074	0.86×10^{-4}	3.183	0.0107	−0.117	1.00×10^{-4}

TABLE 3. Maximum growth rate for resonances $n=4, 5$. The unperturbed waves have the same value $a/h=0.05$ for various depths.

for the growth rate. Between the two regions, the growth rate is very small and the band reduces practically to a line of infinitesimal thickness. Thus, only one local maximum growth rate was found by Bryant (1978) for an unstable oblique disturbance with $\kappa\approx0.3$. With the shallow-water scalings, Bryant (1978) reported that the most unstable disturbance has $\mathrm{Im}(\sigma_B)=2.65\times10^{-3}$. In our study, a local maximum growth rate is found in the same region, but for an unstable mode with $\kappa=0.22$ near $(p,\ q)\approx(0.2, 0.092)$ and with $\mathrm{Im}(\sigma_B)=2.99\times10^{-3}$. However, the most unstable disturbance of class I ($n=2$) is not oblique, but almost parallel to the basic wave. The growth rate of this disturbance near $(p, q)=(1.112,\ 0.015)$ is $\mathrm{Im}(\sigma_B)=1.01\times10^{-2}$, or with our scalings $\mathrm{Im}(\sigma)=3.57\times10^{-4}$. The present differences with Bryant's analysis can be explained, because he used a truncated form of the equations of motion both for the computation of the nonlinear wave and for the linear stability analysis. It is well-known that the latter problem is very sensitive to the accuracy of the nonlinear wave computations. We use the full exact equations of motion and linearize the perturbations about the nonlinear unperturbed wave and not about the flat surface as Bryant (1974, 1978).

Figure 3 shows the bands of instability associated with the resonances $n=2,\ 3,\ 4$ for the same depth. All the bands of instability are located in the vicinity of their corresponding linear resonance curves. For class II ($n=3$), all instabilities on the axis $p=1/2$ are phase-locked [$\mathrm{Re}(\sigma)=0$] with the unperturbed wave. For class I ($n=4$), all instabilities on the axis $p=0$ are also phase-locked with the unperturbed wave. The most unstable mode of the class II ($n=3$) is located on the axis $p=1/2$, while for the class I ($n=4$) it is on the axis $p=0$. The characteristics of the most unstable disturbance of each resonance are reported in tables 2 and 3.

Both bands of class II ($n=3$) and class I ($n=4$) instabilities consist of two domains bound by an infinitesimal band with extremely small growth rates. Following Stiassnie & Shemer (1984), the first region associated with low values of p will be referred to as the primary region of instability, and the other associated with

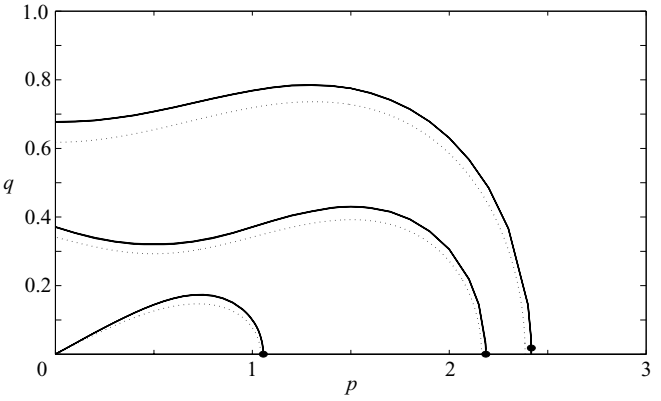

FIGURE 4. As figure 3, but for $h = 0.3$.

large values of p as the secondary region of instability. These authors observed disconnections between the two domains of class I ($n = 2$) instabilities and, sometimes, disappearance of the secondary region. Since these features were not observed in McLean (1982*b*) who used the full equations, they speculated that it could result from the errors introduced by their perturbation approach. Besides, Stiassnie & Shemer (1984) have found that the secondary region of instability of the class I ($n = 2$) could have greater growth rates than the corresponding primary region for $0.37 \leqslant h \leqslant 0.85$. This occurs for small to moderate amplitude, and is in agreement with McLean's result for $h = 0.5$. Namely, the most unstable disturbance for class I ($n = 2$) is located in the secondary region for $ak = 0.10$ and is quasi-two-dimensional. For all the cases we have considered, except for $h = 0.1$ and $n = 2$, our numerical results indicate that there always exist a primary and secondary region for each resonance. However, we have never observed disconnections between the two domains of one particular band of instability.

Figure 4 shows the regions of unstable disturbance for the second permanent wave with $a/h = 0.05$ and $h = 0.3$. For this wave, the dominant instability is still associated with the second-order resonance, i.e. class I ($n = 2$), and is two-dimensional. Nevertheless, the main difference from the first wave concerns the instabilities associated with resonances $n = 3$, 4. Indeed, the instabilities located in the secondary region of class II ($n = 3$) have greater local growth rates than those of the instabilities, which are located in the primary region. On the other hand, the local maximum growth rate in the primary region is still located on the axis $p = 1/2$ and phase-locked to the unperturbed wave, while that of the secondary region is located near $(p, q) = (2.185, 0)$ which corresponds to a two-dimensional disturbance. Similarly, for class I ($n = 4$), the corresponding region of instabilities also consists of two domains, yet with comparable local maximum growth rates. The most unstable mode of the primary region is located on the axis $p = 0$ and phase-locked to the unperturbed wave, with $\mathrm{Im}(\sigma) = 0.8301 \times 10^{-4}$ or with Bryant's scalings $\mathrm{Im}(\sigma_B) = 3.00 \times 10^{-3}$. The second local maximum growth rate is in the secondary region, near $(p, q) = (2.417, 0.018)$, and has a slightly greater value, i.e. $\mathrm{Im}(\sigma) = 0.8408 \times 10^{-4}$ or $\mathrm{Im}(\sigma_B) = 3.01 \times 10^{-3}$. The characteristics of the dominant instabilities are given in tables 2 and 3.

For the third wave $a/h = 0.05$ and $h = 0.25$, figure 5 shows that the most unstable modes of each resonance are in the corresponding secondary regions, and represent quasi-two-dimensional instabilities. In this case, the dominant unstable mode corresponds to a class II ($n = 3$) instability; see tables 2 and 3. We note that

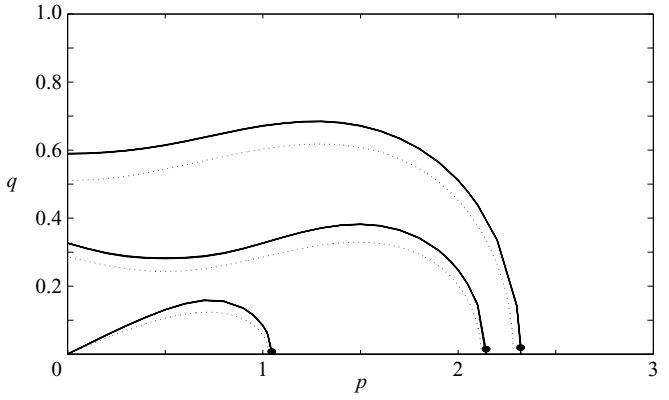

FIGURE 5. As figure 3, but for $h = 0.25$.

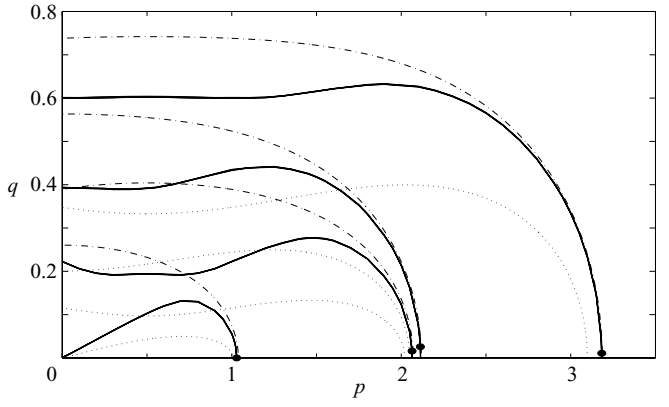

FIGURE 6. Diagram of instability for $a/h = 0.05$ and $h = 0.1$. Unstable regions for the resonances $n = 2, 3, 4, 5$. The dots label the most unstable modes of each region of instabilities. The dotted lines represent the resonance curves and the dashed-dotted lines the nonlinear resonance curves.

the maximum growth rate of the class I ($n = 4$) instabilities is greater than that of the class I ($n = 2$) instabilities. In the primary region of instability associated with the resonances $n = 3$, 4, the most unstable perturbations are all phase-locked with the unperturbed wave. These instabilities are located on the axis $p = 1/2$ for class II ($n = 3$) and on the axis $p = 0$ for class I ($n = 4$). They represent unstable three-dimensional disturbances. Yet, their growth rate is lower than that of the instabilities in the secondary region.

For the fourth wave $a/h = 0.05$ and $h = 0.1$, the most unstable perturbations are two-dimensional or quasi-two-dimensional as shown in figure 6. The dominant unstable mode corresponds to a class II ($n = 5$) instability. Similarly, most unstable disturbances in the primary region are all phase-locked with the unperturbed wave. For class II ($n = 3, 5$), these are located on the axis $p = 1/2$, and on the axis $p = 0$ for class I ($n = 4$). Bryant (1978) has commented briefly on this case. He found oblique instabilities only in the primary region of class I ($n = 2$) instabilities with smaller growth rates than in the cases $h = 0.5$ and $h = 0.25$. Our numerical results indicate that there is only one local maximum growth rate for the class I ($n = 2$) instabilities located in the secondary region where $p > 1$ and $q \ll 1$. The most unstable disturbance is quasi-two-dimensional with $(p, q) = (1.0457, 0.0079)$ and $\mathrm{Im}(\sigma_B) = 2.11 \times 10^{-2}$. In the

primary region, the growth rates are consistent with Bryant's results, i.e. a decrease of the growth rates with decreasing depth, although there is no longer local maximum growth rate in this region.

We note that in the two previous cases, the instability bands for all resonances move further from their corresponding resonance curve as the depth decreases. Formally, the resonance curves are still applicable for finding the unstable regions, but for an infinitesimal amplitude of the basic wave with frequency given by the linear dispersion relation, $c_0 = \sqrt{\tanh(h)}$. They are useful in very shallow water if $ak \ll (kh)^3$ holds, in accordance with the Stokes' expansions approach. For $a/h < 0.05$, we have found that the bands of instabilities are extremely thin and the growth rates extremely small. For $a/h > 0.05$ and $h \leqslant 0.3$, we have found it practical to replace c_0 by c, the speed of the basic wave, in the linear resonance conditions (2.22)–(2.23), in order to locate the secondary region of instabilities of class I,

$$\sqrt{k_m \tanh(k_m h)} + \sqrt{k_{-m} \tanh(k_{-m} h)} = 2mc, \tag{3.1}$$

and of class II,

$$\sqrt{k_m \tanh(k_m h)} + \sqrt{k_{-m-1} \tanh(k_{-m-1} h)} = (2m+1)c. \tag{3.2}$$

Figure 6 illustrates how the secondary region of instabilities develops around the nonlinear resonance curves (3.1)–(3.2) where $q \ll 1$. However, it is important to notice that these nonlinear resonance curves move in the (p, q)-plane as the amplitude of the basic wave varies. Moreover, their use is limited to quasi-two-dimensional disturbances. This is important since we have found that the dominant instabilities are quasi-two-dimensional when the depth decreases.

For the shallow-water cases $h \leqslant 0.3$, we have found that the first-order cnoidal approximation is practical for estimating the amplitude correction of the phase speed. The KdV cnoidal wave theory predicts in dimensional form

$$c_{KdV} = \sqrt{gh} \left[1 - \frac{a}{h} + \frac{1}{m} \frac{2a}{h} \left(1 - \frac{3E(m)}{2K(m)} \right) \right], \tag{3.3}$$

in terms of the elliptic parameter m, where $K(m)$ and $E(m)$ are, respectively, the complete elliptic integrals of the first and second kind. Using c_{KdV}, after normalization, instead of the exact value c, produces the same nonlinear resonance curves. However, this theory is valid when $a/h \ll 1$ with $a/h \sim (kh)^2$. For large values of the parameter $(a/h)/(kh)^2$, the KdV model diverges from the exact phase velocity c, because it underestimates the amplitudes of the higher harmonics of the basic wave when $(a/h)/(kh)^2$ increases, as explained in Bryant (1974).

In summary, we have found that when the depth decreases, for a fixed shallow-water amplitude $a/h = 0.05$, the dominant instabilities corresponding to the resonances $n = 2, 3, 4$ and 5 become quasi-two-dimensional and are shifted in the secondary region. The results concerning the resonances $n = 2, 3$ are consistent with previous weakly nonlinear predictions of Bryant (1978), McLean (1982*b*) and Stiassnie & Shemer (1984). Higher-order resonances dominate in the two shallowest cases we have studied. The order of the resonance associated with the maximum growth rate of all instabilities is found to increase with decreasing depth. Comparison of the growth rates for the various instabilities is given in tables 2 and 3.

3.2. *Results for moderate- and large-amplitude waves*

The case $h = 0.5$ has already been investigated by McLean (1982*b*) for different values of the steepness. In his work, the wave steepness ranges from small amplitude

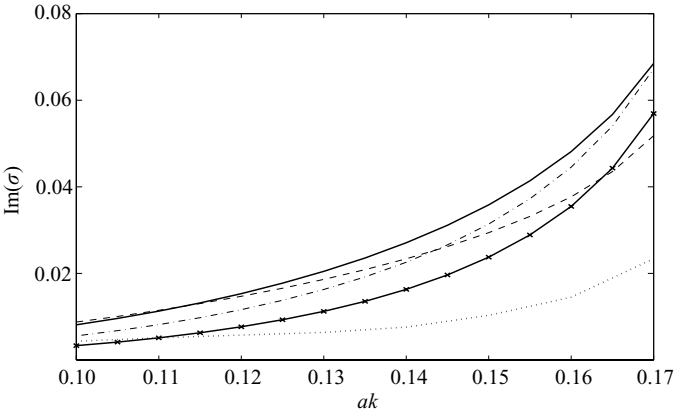

FIGURE 7. Maximum growth rate of class I and class II instabilities for $h = 0.5$ as a function of wave steepness. $\cdots$, class I ($n = 2$); - - -, class II ($n = 3$); —, class I ($n = 4$); –·–, class II ($n = 5$); —x—, class I ($n = 6$).

up to $ak = 0.160$ which is roughly 85 % of the maximum wave steepness equal to 0.188 (see Cokelet 1977). The results concern the instabilities associated with class I ($n = 2$) and class II ($n = 3$). He found that the instabilities of class I are essentially three-dimensional. The main discovery for this class is that, for small steepness the most unstable mode is two-dimensional with a wavelength comparable with that of the basic nonlinear wave; for higher steepness it becomes three-dimensional. More importantly, two-dimensional long-wavelength perturbations are found to be stable for this depth and for the range of steepness considered. Finally, McLean (1982*b*) reported that the behaviour of class II instabilities was analogous to the deep-water case, as well as to the finite-depth case, that is, they are essentially three-dimensional and dominate the class I instabilities for sufficiently large steepness. We extended the computations to higher steepness, and found that the results of McLean (1982*b*) are incomplete, even for steepness lower than $ak = 0.160$.

For $ak \lesssim 0.112$, the dominant instabilities belong to the lowest-order resonance of the class II ($n = 3$). The most unstable mode is three-dimensional occurring at $p = 1/2$ and $q \neq 0$, and is phase-locked to the unperturbed nonlinear wave [$\mathrm{Re}(\sigma) = 0$]. For $ak \geqslant 0.112$, we found that the instabilities associated with the next-order resonance of class I ($n = 4$) are always dominant, as far as the most unstable mode is of interest. The most unstable mode is always a three-dimensional perturbation and occurs on the q-axis ($p = 0$). Thus by definition, it is a three-dimensional perturbation with the same longitudinal periodicity as the unperturbed wave (in the x-direction). This was not observed by McLean (1982*b*) who restricted his analysis to class I ($n = 2$) and class II ($n = 3$), the lowest-order resonances.

For higher steepness, the maximum growth rates of the higher-order resonances ($n = 5, 6$) also become important, although lower than that of class I ($n = 4$). This is shown in figure 7. Meanwhile, the corresponding instability regions grow in the wave vector space of the perturbation, as shown in figures 8 and 9. The most unstable mode of class II ($n = 5$) is three-dimensional, occurring at $p = 1/2$ and $q \neq 0$, and is also phase-locked to the unperturbed wave. As for class I ($n = 4$), the most unstable mode of class I ($n = 6$) is located on the q-axis and is also phase-locked to the unperturbed wave. Besides the shifting from two-dimensional to three-dimensional of the most unstable mode of class I ($n = 2$), the most unstable mode of each resonance shifts

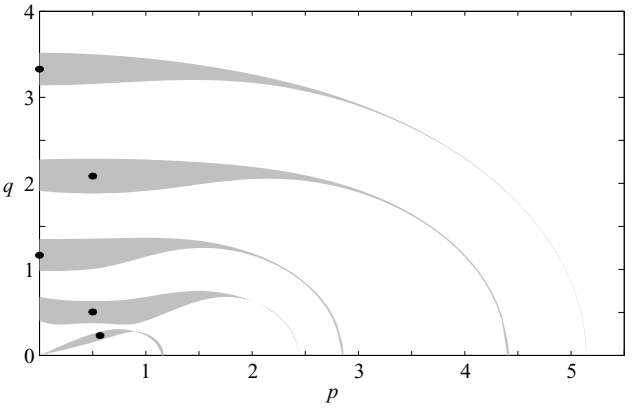

FIGURE 8. Instability regions of class I and class II for $ak = 0.160$ and $h = 0.5$. The dashed-dotted lines represent the resonance curves. The dots label the most unstable modes of each region of instabilities.

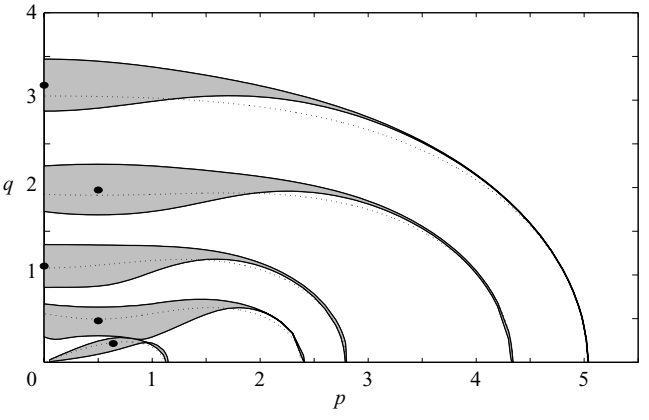

FIGURE 9. As figure 8, but for $ak = 0.170$.

towards its corresponding linear resonance curve as the steepness becomes very large (see figure 9).

For the case with $h = 0.3$, the maximum wave steepness is equal to 0.118. The computations show that from small to moderate steepness, the maximum growth rates of the instabilities associated with the resonances $n = 3, 4, 5$ and 6 are close to each other (see figures 10 and 11). For $0.25 < ak < 0.061$, the dominant instability is three-dimensional and of class I ($n = 4$). Note that for $ak = 0.050$, the most unstable mode of class I ($n = 2$) is two-dimensional, as shown in figure 12. For this class, we have found that the shift from two-dimensional to three-dimensional of the most unstable disturbance occurs between $ak = 0.080$ and $ak = 0.090$. For $0.061 < ak < 0.095$, the dominant instability is still three-dimensional, but is associated with the next-order resonance, class II ($n = 5$). It is located on the axis $p = 1/2$. Figure 11 shows that as the steepness of the basic wave increases, when $ak > 0.095$, the most unstable mode of class I ($n = 6$) instabilities becomes dominant. This mode is located on the axis $p = 0$. In fact, the growth rates of the instabilities associated with the high-order resonances $n = 5, 6$ and 7 are greater than those of the resonances $n = 2, 3$ and 4 when $ak > 0.090$. For very high steepness, we see that instabilities of class I ($n = 6$) should

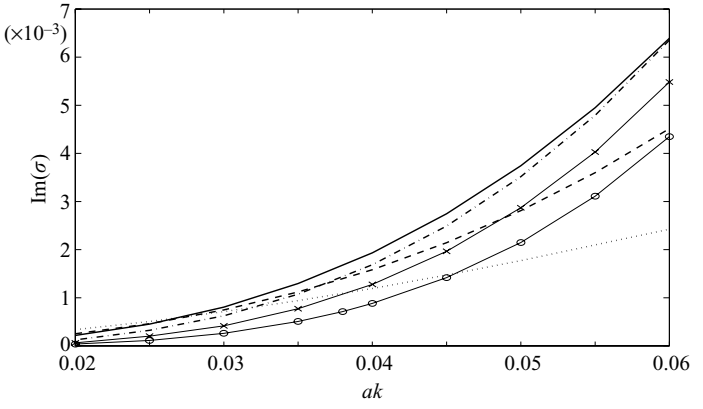

FIGURE 10. Maximum growth rate of class I and class II instabilities for $h = 0.3$ as a function of wave steepness. ···, class I ($n = 2$); - - -, class II ($n = 3$); —, class I ($n = 4$); –·–, class II ($n = 5$); —x—. class I ($n = 6$); —o—, class II ($n = 7$).

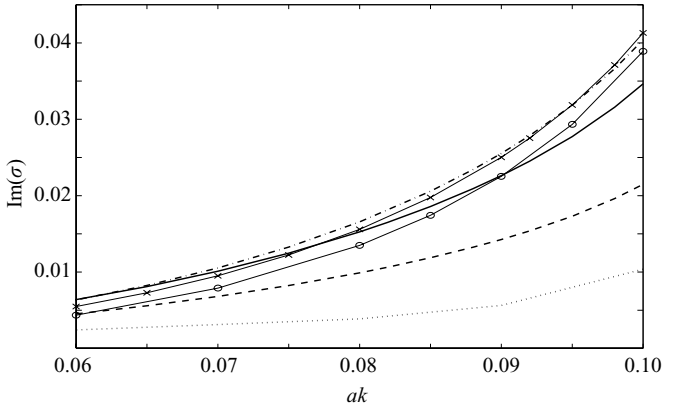

FIGURE 11. As figure 10 but for larger values of the wave steepness.

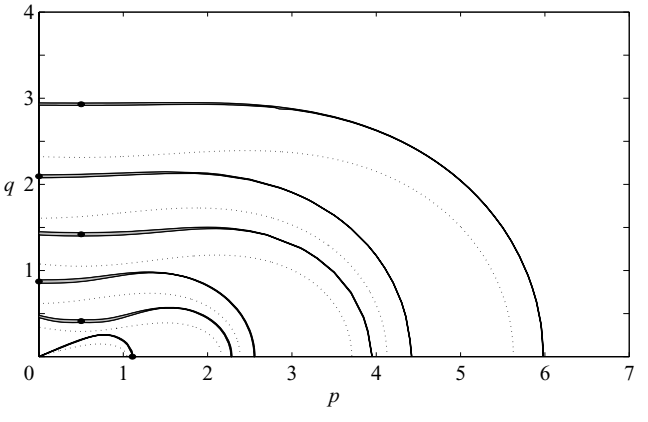

FIGURE 12. Instability regions of class I and class II for $ak = 0.050$ and $h = 0.3$. The dashed-dotted lines represent the resonance curves. The dots label the most unstable modes of each region of instabilities.

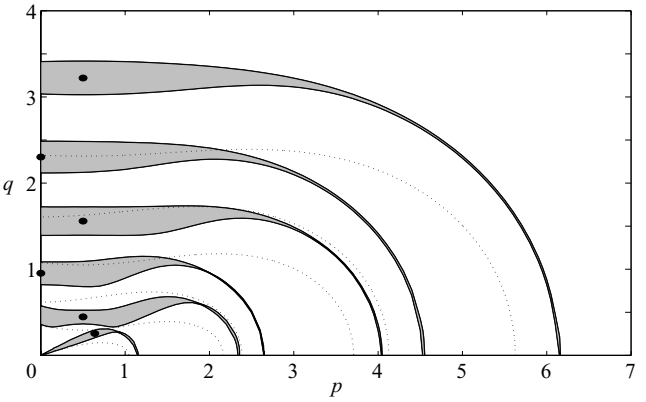

FIGURE 13. As figure 12, but for $ak = 0.100$.

be the dominant instabilities. For $ak = 0.100$, the dominant instability, namely that of class I ($n = 6$), corresponds to disturbances with the same longitudinal periodicity as shown in figure 13. Hence, 8-wave interactions are dominant for such large steepness.

3.3. *Three-dimensional stationary disturbances*

In this subsection, we consider marginally stable disturbances ($\sigma = 0$) of the nonlinear periodic progressive waves associated with instabilities of class I ($n = 4, 6$) and class II ($n = 3, 5, 7$). In fact, it is well known that for gravity waves in deep water, the most unstable disturbances of class II ($n = 3$), which are located on the axis $p = 1/2$ and phase-locked to the unperturbed wave, lead when dominant for $ak > 0.3$ to the formation of three-dimensional waves of permanent form with surface patterns symmetric about the direction of propagation. These waves were observed experimentally by Su *et al.* (1982), and their characteristics were in agreement with numerical bifurcation predictions obtained with the exact equations by Meiron, Saffman & Yuen (1982). For small steepness and very oblique modulational perturbations, the bifurcation predictions also agree with similar predictions obtained by Saffman & Yuen (1980) who used the Zakharov equation. The latter authors have demonstrated that there exist an infinity of loci (p, q) representing stationary oblique disturbances, which can bifurcate into two branches of new solutions either symmetric about the direction of propagation or skewed. Yet, the skew solutions have never been calculated, within the exact equations, and the selection mechanism for its occurrence remains an open question. In this subsection, attention is drawn to steady three-dimensional patterns obtained by superposing a marginally stable stationary disturbance on the basic wave.

For a given undisturbed depth kh and steepness ak, there exists an infinity of marginally stable modes for each class of instabilities ($n > 2$). As discussed by Saffman & Yuen (1985), bifurcations can occur when a marginally stable disturbance can be superposed on a steady wave. For a given value of the wave steepness, this is possible on an infinite number of loci in the (p, q)-plane (see dashed lines on figure 2 of McLean 1982*a*).

We have shown that the dominant instabilities are three-dimensional for moderate to large steepness as the water depth decreases. They are located on the axis $p = 0$ for class I and on the axis $p = 1/2$ for class II. Thus, we focus on the marginally stable disturbances which are located at the boundaries of the corresponding unstable region for $p = 0$ or $p = 1/2$. This suggests for each class of instability the existence of two

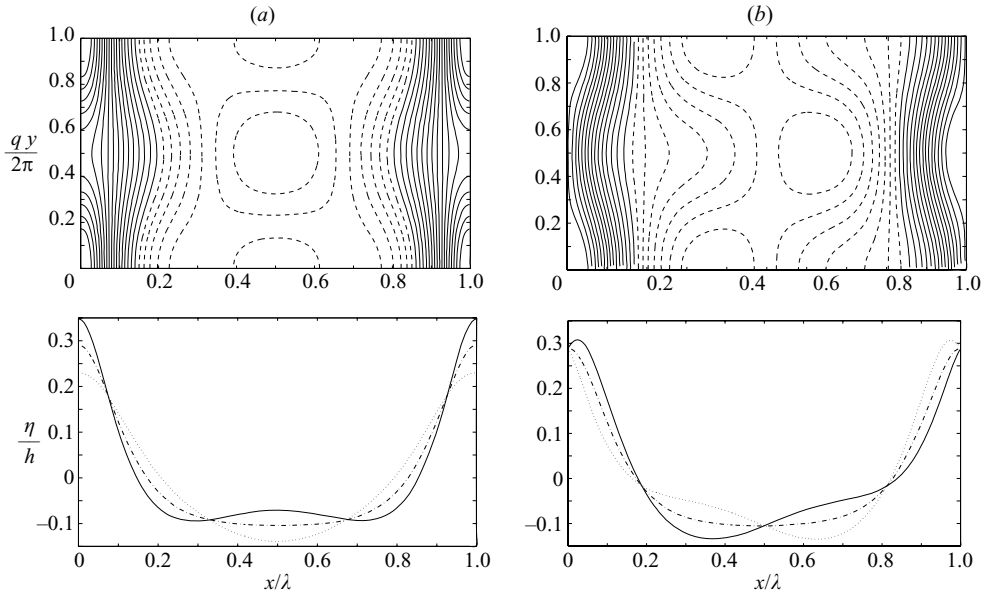

FIGURE 14. The unperturbed wave corresponds to $h = 0.5$ and $ak = 0.100$. Top: Surface-contour plot of bifurcated gravity wave; bottom: cuts through the corresponding surface at: —, $y = 0$; —·—, $y = \pi/2q$; . . . , $y = \pi/q$. (*a*) $q = 1.205$ ($p = 0$, lower intersection); (*b*) $q = 1.277$ ($p = 0$, upper intersection).

types of three-dimensional wave symmetric about their direction of propagation. In the following sections, we consider symmetric three-dimensional waves by superposing on the undisturbed nonlinear wave the computed three-dimensional marginally stable mode associated with the dominant class of instability. These three-dimensional waves will be referred to as bifurcated waves, although it should be more rigorous to use a bifurcation technique to calculate the different bifurcated solutions. The eigenfunctions (2.18) and (2.19) are normalized so that the maximum crest-to-trough height of the disturbance is 0.3 times the crest-to-trough height of the undisturbed nonlinear wave.

3.3.1. *Stationary disturbances of class I ($n = 4, 6$)*

It has been found that all instabilities of class I ($n = 4, 6$) have eigenvalues with zero real part on the axis $p = 0$. Thus, the stationary modes of class I ($n = 4, 6$) at the boundary of the unstable region with $p = 0$ may lead to three-dimensional waves that are doubly periodic in two orthogonal directions. The longitudinal wavelength of these disturbances is the same as that of the undisturbed wave and the transverse wavelength is equal to $2\pi/q$. They can be considered as a type of spontaneous short-crested waves arising as superharmonic bifurcations from the undisturbed two-dimensional wave.

We consider a wave steepness $ak = 0.1$ to illustrate the bifurcated wave from stationary perturbations of class I ($n = 4$) in the case $h = 0.5$, although these modes are not associated with the dominant instabilities. Indeed, we have found that the most unstable mode of class II ($n = 3$) is the dominant instability with $\mathrm{Im}(\sigma) = 8.77 \times 10^{-3}$. The growth rate of the most unstable mode of class I ($n = 4$) is $\mathrm{Im}(\sigma) = 8.12 \times 10^{-3}$, which is rather close to the dominant growth rate of that of class II ($n = 3$). However, we take the stationary modes of class I ($n = 4$), with $p = 0$, mainly for qualitative information about the bifurcated surface patterns. Figures 14(*a*) and 14(*b*) show the

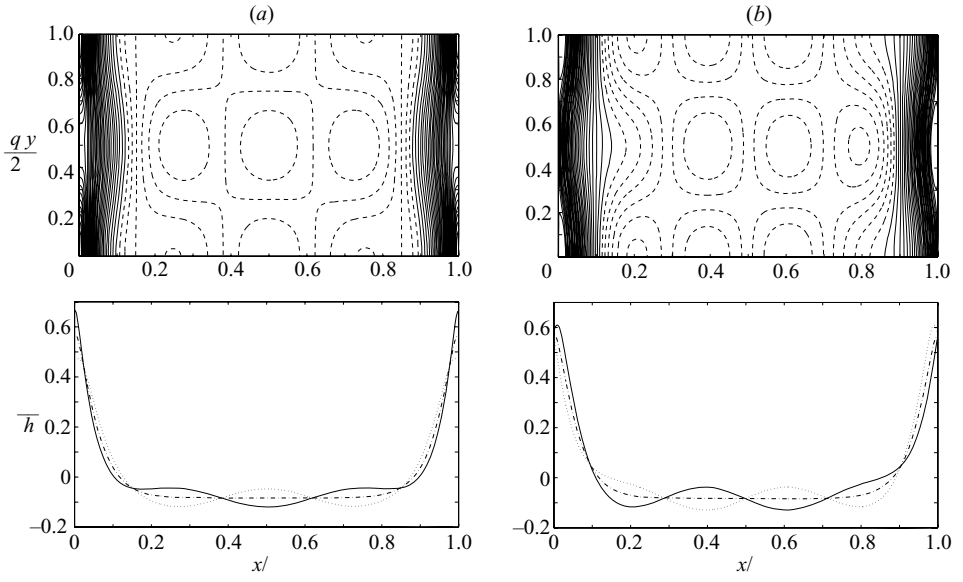

FIGURE 15. As figure 14, but for $h = 0.3$; (*a*) $q = 2.119$, (*b*) $q = 2.485$.

surface-contour plot and cuts at $y = 0, \pi/2q, y\pi/q$ corresponding to the bifurcations from stationary disturbances at the boundary of the unstable region of class I ($n = 4$), respectively, for the lower ($q = 1.205$) and the upper ($q = 1.277$) intersections with the axis $p = 0$. For $h = 0.3$ and $ak = 0.100$, the instabilities of class I ($n = 6$) are dominant. Figures 15(*a*) and 15(*b*) characterize the bifurcated waves corresponding, respectively, to the stationary modes of class I ($n = 6$) at the lower intersection ($q = 2.119$) and at the upper intersection ($q = 2.485$).

From the examination of the wave patterns, we can see that all these waves are symmetric about the direction of propagation of the basic wave. However, three-dimensional waves considered for the lower intersections have one more axis of symmetry which is perpendicular to the first one. Besides, this axis of symmetry can be invariantly considered at the crest ($x = 0$) or at the trough ($x = \pi$) of the bifurcated waves. These symmetries are lost for bifurcated waves considered for the upper intersection. These waves remain only symmetric about their direction of propagation.

3.3.2. *Stationary disturbances of class II ($n = 5, 7$)*

It has been found that all instabilities of class II ($n = 5, 7$) have eigenvalues with zero real part on the axis $p = 1/2$. The bifurcated waves correspond to subharmonic bifurcations, which have a longitudinal wavelength equal to twice that of the two-dimensional unperturbed wave. These waves are doubly periodic in the two orthogonal directions. Their transverse wavelength is equal to $2\pi/q$.

For $h = 0.3$ and $ak = 0.08$, the instabilities of class II ($n = 5$) are dominant. Figures 16(*a*) and 16(*b*) characterize the bifurcated waves corresponding to the stationary modes of class II ($n = 5$), respectively, at the lower intersection ($q = 1.491$) and at the upper intersection ($q = 1.640$) between the boundary region and the axis $p = 1/2$. These surface patterns have similar characteristics to that of the symmetric three-dimensional bifurcations of Stokes waves in deep water, although a richer transverse structure characterizes the presented higher-order bifurcations of class II

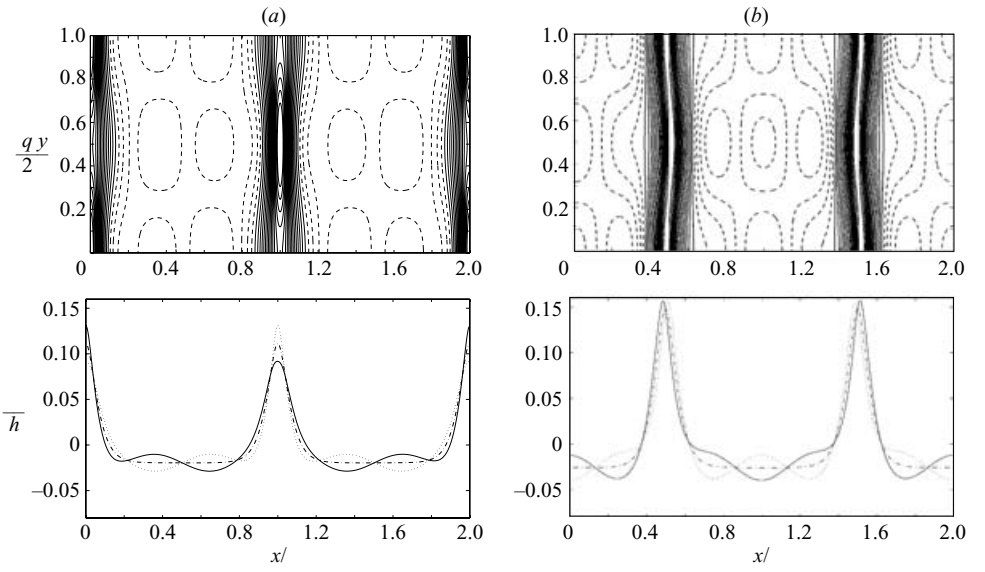

FIGURE 16. As figure 14, but for $h = 0.3$, $ak = 0.080$; (*a*) $q = 1.491$ ($p = 1/2$, lower intersection), (*b*) $q = 1.640$ ($p = 1/2$, upper intersection).

($n = 5, 7$). From the lower intersections, the symmetric bifurcated waves have one more axis of symmetry, which passes through the crest and is perpendicular to the direction of propagation. In deep water, these waves are referred to as crest-symmetric three-dimensional waves. They arise from the lower stationary mode of class II ($n = 3$) instabilities with $p = 1/2$. The bifurcated waves that arise from the upper stationary modes are referred to as trough-symmetric three-dimensional waves, since the secondary axis of symmetry passes through the trough ($x = 2\pi$) of the bifurcated wave with period doubling. Thus, the secondary symmetry is not lost for these stationary modes. Similar properties are observed for the presented bifurcated waves from stationary modes of class II ($n = 5, 7$).

4. Conclusion and discussion

A study of three-dimensional instabilities of two-dimensional periodic gravity waves in shallow water has been presented. The stability analysis has extended and supplemented work by Bryant (1974, 1978), Stiassnie & Shemer (1984) and McLean (1982*b*) to shallower water depths and steeper basic waves.

For dimensionless depths $h < 0.5$, weakly nonlinear two-dimensional water waves are found to be most unstable to two-dimensional or quasi-two-dimensional disturbances. The maximum growth rate of each class is found in the secondary region of instability with $p > 1$, in the (p, q)-plane. For $h = 0.5$, the maximum growth rates correspond to three-dimensional instabilities in the primary region except for the class I ($n = 2$) whose dominant instabilities are two-dimensional or quasi-two-dimensional in the secondary region of instability, close to $p = 1$. The case restricted to four-wave interactions, was investigated by Bryant who found the most unstable infinitesimal perturbation to be oblique, i.e. fully three-dimensional. This is because he limited his study to small values of the perturbation wavenumber. Comparing numerically the nonlinear evolutions of the most unstable perturbation and linearly stable perturbations parallel to the basic wave, he observed the dominance of the

parallel disturbances. He explained that the parallel perturbations interact near resonance with all the lower harmonics of the permanent wave, while the oblique disturbances interact resonantly with only the first two harmonics of the permanent wave. To verify this feature, it should be of interest to reiterate the numerical simulations of Bryant by considering as the most unstable perturbation the quasi-two-dimensional and not the fully three-dimensional perturbation. Note that Bryant developed his analysis on the basis of truncated equations. For higher values of the amplitude, class I ($n = 2$) is no more dominant and instabilities of higher order have to be considered. This suggests another kind of perturbations competition.

For moderate to large steepness of the basic wave, the most unstable perturbations belong to the primary regions of instability and are three-dimensional. As a new result it is shown that (i) class I ($n = 4$) becomes dominant for $h = 0.5$ and (ii) class II ($n = 5$) and class I ($n = 6$) predominate successively when increasing the steepness for $h = 0.3$. As the depth h decreases, the number of resonant waves increases. This result is not surprising since for shallow-water waves, the amplitude of the higher-order harmonics is generally more important than in deep water wave trains.

For class I and class II with $n > 3$, we found the most unstable perturbations to be phase-locked to the permanent waves. This suggests new types of steady three-dimensional gravity waves due to bifurcations from two-dimensional to three-dimensional patterns. These patterns correspond to subharmonic bifurcation (period doubling with $p = 1/2$) or superharmonic bifurcation ($p = 0$) for class II and class I, respectively. The computation of the branches of bifurcated solutions is presently underway by using a method of continuation within the framework of the fully nonlinear equations.

The authors are grateful to the reviewers of this paper for their useful comments and suggestions. These have helped us to improve the presentation of this work.

REFERENCES

Benjamin, T. B. 1967 Instability of periodic wave trains in nonlinear dispersive systems. *Proc. R. Soc. Lond.* A **299**, 59–75.

Benjamin, T. B. & Feir, J. E. 1967 The disintegration of wave trains on deep water. *J. Fluid. Mech.* **27**, 417–430.

Benney, D. J. & Roskes, G. J. 1969 Wave instabilities. *Stud. Appl. Maths* **48**, 337–385.

Brinch-Nielsen, U. & Jonsson, I. G. 1986 Fourth order evolution equations and stability analysis for Stokes waves on arbitrary water depth. *Wave Motion* **8**, 455–472.

Bryant, P. J. 1974 Stability of periodic waves in shallow water. *J. Fluid Mech.* **66**, 81–96.

Bryant, P. J. 1978 Oblique instability of periodic waves in shallow water. *J. Fluid Mech.* **86**, 783–792.

Cokelet, E. D. 1977 Steep gravity waves in water of uniform arbitrary depth. *Phil. Trans. R. Soc. Lond.* A **286**, 184–230.

Davey, A. & Stewartson, K. 1974 On three-dimensional wave packets of surface waves. *Proc. R. Soc. Lond.* A **338**, 101–110.

Fenton, J. D. 1979 A high-order cnoidal wave theory. *J. Fluid Mech.* **94**, 129–161.

Hayes, W. D. 1973 Group velocity and nonlinear dispersive wave propagation. *Proc. R. Soc. Lond.* A **332**, 199–221.

Infeld, E. 1980 On three-dimensional generalizations of the Boussinesq and Korteweg–de Vries equations. *Q. Appl. Maths* **38**, 277–287.

Infeld, E. & Rowlands, G. 1979 Three dimensional stability of Korteweg–de Vries waves and solitons. II. *Acta Phys. Polon.* **56**, 329–332.

Infeld, E. & Rowlands, G. 1990 *Nonlinear waves, Solitons and Chaos*, 1st edn. Cambridge University Press.

Longuet-Higgins, M. S. 1988 Lagrangian moments and mass transport in Stokes waves. Part 2. Water of finite depth. *J. Fluid Mech.* **186**, 321–336.

MacKay, R. S. & Saffman, P. G. 1986 Stability of water waves. *Proc. R. Soc. Lond.* A **406**, 115–125.

McLean, J. W. 1982*a* Instabilities of finite-amplitude gravity waves. *J. Fluid Mech.* **114**, 315–330.

McLean, J. W. 1982*b* Instabilities of finite-amplitude gravity waves on water of finite depth. *J. Fluid Mech.* **114**, 331–341.

Meiron, D. I. & Saffman, P. G. & Yuen, H. C. 1982 Calculation of steady three-dimensional deep-water waves. *J. Fluid Mech.* **124**, 109–121.

Saffman, P. G. & Yuen, H. C. 1980 A new type of three-dimensional deep-water wave of permanent form. *J. Fluid Mech.* **101**, 797–808.

Saffman, P. G. & Yuen, H. C. 1985 Three-dimensional waves on deep water. In *Advances in Nonlinear Waves* (ed. L. Debnath), pp. 1–30. Pitman.

Stiassnie, M. & Shemer, L. 1984 On modifications of the Zakharov equation for surface gravity waves. *J. Fluid Mech.* **143**, 47–67.

Su, M.-Y. & Bergin, M. & Marler, P. & Myrick, R. 1982 Experiments on nonlinear instabilities and evolution of steep gravity-wave trains. *J. Fluid Mech.* **124**, 45–72.

Whitham, G. B. 1965 A general approach to linear and nonlinear dispersive waves using a Lagrangian. *J. Fluid Mech.* **22**, 273–283.

Whitham, G. B. 1967 Variational methods and applications to water waves. *Proc. R. Soc. Lond.* A **229**, 6–25.

Zhang, J. & Melville, W. K. 1987 Three-dimensional instabilities of nonlinear gravity–capillary waves. *J. Fluid Mech.* **174**, 187–208.